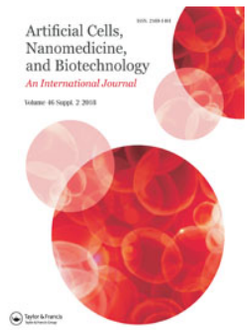

Taylor & Francis
Taylor & Francis Group

Artificial Cells, Nanomedicine, and Biotechnology
An International Journal

ISSN: 2169-1401 (Print) 2169-141X (Online) Journal homepage: https://www.tandfonline.com/loi/ianb20

In vivo evaluation of the combination effect of near-infrared laser and 5-fluorouracil-loaded PLGA-coated magnetite nanographene oxide

Arezoo Mohammadi Gazestani, Samideh Khoei, Sepideh Khoee, Soraya Emamgholizadeh Minaei & Manijeh Motevalian

To cite this article: Arezoo Mohammadi Gazestani, Samideh Khoei, Sepideh Khoee, Soraya Emamgholizadeh Minaei & Manijeh Motevalian (2018) *In vivo* evaluation of the combination effect of near-infrared laser and 5-fluorouracil-loaded PLGA-coated magnetite nanographene oxide, Artificial Cells, Nanomedicine, and Biotechnology, 46:sup2, 25-33, DOI: 10.1080/21691401.2018.1450265

To link to this article: https://doi.org/10.1080/21691401.2018.1450265

ARTIFICIAL CELLS, NANOMEDICINE, AND BIOTECHNOLOGY
2018, VOL. 46, NO. S2, S25–S33
https://doi.org/10.1080/21691401.2018.1450265

In vivo evaluation of the combination effect of near-infrared laser and 5-fluorouracil-loaded PLGA-coated magnetite nanographene oxide

Arezoo Mohammadi Gazestani[a], Samideh Khoei[a,b], Sepideh Khoee[c], Soraya Emamgholizadeh Minaei[a] and Manijeh Motevalian[b,d]

[a]Department of Medical Physics, School of Medicine, Iran University of Medical Sciences, Tehran, Iran; [b]Razi Drug Research Centre, Iran University of Medical Sciences, Tehran, Iran; [c]Department of Polymer Chemistry, School of Sciences, University of Tehran, Tehran, Iran; [d]Department of Pharmacology, School of Medicine, Iran University of Medical Sciences, Tehran, Iran

ABSTRACT

Magnetite nanographene oxide has exhibited great potential in drug delivery and photothermal therapy (PTT) for cancer treatment. Here we developed 5-fluorouracil-loaded poly (lactic-co-glycolic acid)-coated magnetite nanographene oxide (NGO-SPION-PLGA-5-Fu) to simplify combined PTT and chemotherapy in one complex. The nanocarrier was synthesized using a modified $O_1/W_1/O_2/W_2$ multiple emulsion solvent evaporation method and was characterized for size, zeta potential, drug loading, *in vitro* and *in vivo* release. In this paper, *in vivo* suppression effect of PTT and chemotherapy using this synthesized magnetite nanographene oxide was studied. The *in vitro* release of 5-Fu from nanoparticles showed that 41.36% of the drug was released within 24 h. *In vivo* release showed that 5-Fu has a sustained release profile and prolonged lifetime in the rabbit plasma. Remarkably, a single injection of NGO-SPION-PLGA-5-Fu and 808 nm near-infrared laser (NIR) irradiation for 3 min effectively suppressed the growth of tumours compared with 5-Fu alone ($p < .01$). Magnetic resonance imaging (MRI) confirmed that the magnetic nanographene oxide was effectively targeted to the tumour site. Therefore, NGO-SPION-PLGA-5-Fu showed excellent PTT efficacy, magnetic targeting property, and MRI ability, indicating that there is a great potential of NGO-SPION-PLGA-5-Fu for cancer theranostic applications.

ARTICLE HISTORY
Received 19 January 2018
Revised 5 March 2018
Accepted 6 March 2018

KEYWORDS
5-Fluorouracil; magnetite nano-graphene oxide; photothermal therapy; magnetic targeting; PLGA; colon cancer

Introduction

Recently, hyperthermia (41–45 °C) has proven to have synergistic effects with traditional treatments such as chemotherapy and radiotherapy [1]. Despite limited selectivity (to cancer cells) of chemotherapy, which could lead to unexpected side effects to normal tissues [2], a combination of chemotherapy and PTT is able to destroy cells as a minimally invasive treatment methodology [3]. PTT is a local treatment and only the area exposed to light is treated [4]. It is expected that the effects of simultaneous chemotherapy and heating on tumour cells can enhance the therapeutic gain; also anticancer efficiency can significantly improve with targeted chemotherapy and drug delivery to the specific tumour region [5].

The fundamental characteristics of heating are denaturation of cell proteins and increasing cell membrane permeability, which is satisfactory for the penetration of drugs into tissues [6]. Nowadays, more studies are focused on NIR-absorbing photothermal agents to attend as heat carriers for hyperthermia [7–10]. These materials, such as carbon nanotubes, gold nanomaterials and graphene, can strongly absorb NIR light and convert it to heat energy to kill cancer cells without affecting healthy tissues [11].

Recently, graphene-based nanomaterials have also attracted interest in the field of biomedicine as they have proven to be great candidates for drug and gene delivery [12], and cancer phototherapies [13].

Graphene oxide (GO) sheets with outstanding high specific surface area can interact with various biomolecules for the application of *in vitro* and *in vivo* drug delivery [14]. Because it has a high surface area and polyaromatic surface structure, the loading capacity of nanographene oxide (NGO) is significantly sufficient [15,16]. Moreover, the photothermal sensitivity of NGO and its optical absorption in the NIR region is higher than in carbon nanotubes, which leads to photothermal ablation of tumours [10,17]. Additionally, because they are hydrophilic groups on both sides of NGO they confirm good stability and solubility in physiological solutions [18].

Nevertheless, the major drawback of GO is its toxicity in biological systems [19]. To overcome this problem, nanoscale GO is prepared with biocompatible coating such as poly (lactic-co-glycolic acid) [20]. Much interest has been concentrated on preparation of biodegradable and biocompatible PLGA nanomaterials, owing to their potential utility in reducing enzymatic degradation, encapsulation and sustained release of various drugs, and higher drug payload and because they

CONTACT Samideh Khoei khoei.s@iums.ac.ir, skhoei@gmail.com Department of Medical Physics, School of Medicine, Razi Drug Research Centre, Iran University of Medical Sciences, P.O. Box: 1449614525, Tehran, Iran

do not induce immune reactions or inflammation, increasing efficacy of the treatment [21,22]. The US Federal Drug Agency has approved the use of PLGA in medical applications. In the body, PLGA hydrolyses into the natural and biodegradable metabolites lactic acid and glycolic acid, resulting in minimal systemic toxicity [23,24].

5-Fluorouracil is a pyrimidine analogue of the antimetabolite anticancer drug class which is used in the treatment of solid tumours such as colon cancer [25]. Wide distribution, non-selectivity effect, and short plasma circulation half-life (8–20 min) of 5-Fu result in side effects and poor therapeutic efficacy [26]. Therefore, 5-Fu was loaded onto the biodegradable polymers or graphene sheets to extend its life time [27].

Dramatically, super paramagnetic iron oxide nanoparticles (SPIONs), due to their special magnetic properties [28], biocompatibility, chemical stability and relatively non-toxic nature (in the body, SPIONs are metabolized into oxygen and elemental iron by hydrolytic enzymes, where the iron accumulates into the natural body stores) [29], have been applied in many fields of biomedicine, such as magnetic resonance imaging (MRI) contrast enhancement [30–32], targeted drug delivery [33] and hyperthermia treatment of cancer [34].

The increasing use of core-shell nanoparticles with highly controlled optical and magnetic properties has created good attention for therapeutic applications and diagnosis (theranostic agents) [35]. The GO–super paramagnetic iron oxide nanoparticle (GO–SPION) composite has attracted extensive attention because of its potential as a contrast agent for cell labelling in MRI [36]. SPIONs produce strong hypointense T2-weighted signal in MRI, which lead to non-invasive monitoring treatment response [37]. Moreover, active magnetic targeting (by applying an external magnetic field) and PTT treatment using SPIONs enhance the sensitivity and specificity of the therapy [38].

To address these issue, in this study, a stepwise synthetic method was designed to create a nanocomplex of NGO-SPION, which was modified with a biocompatible polymer, PLGA and used as the carrier for loading and delivery of 5-fluorouracil with the aim to achieve highly efficient cancer chemotherapy and PTT with minimal side effects in *in vivo* applications.

Materials and methods

Materials

Graphite powder, 5-fluorouracil, potassium permanganate ($KMnO_4$), and phosphoric acid (H_3PO_4) were purchased from Sigma Chemical Company. Poly (lactic-co-glycolic acid) (PLGA) was prepared from Boehringer-Ingelheim. Hydrogen peroxide (H_2O_2), sulphuric acid (H_2SO_4), hydrochloric acid (HCl), iron (II) chloride tetrahydrate ($FeCl_2.4H_2O$), iron (III) chloride hexahydrate ($FeCl_3.6H_2O$), oleic acid, ammonia solution (25 vol%), dichloromethane, glycerine, Span60 and Tween60 were purchased from Merck Chemical Company.

Cell culture materials such as Roswell Park Memorial Institute (RPMI) 1640, penicillin–streptomycin solution, foetal bovine serum (FBS), and Trypsin-EDTA (0.25%) were obtained from Gibco. Mouse colon cancer cell line CT26 and Male BALB/c mice were provided from Pasteur Institute of Iran.

Synthesis of magnetic NGO–PLGA-5-Fu

NGO-SPION-PLGA-5-Fu nanoparticles were prepared using a modified $O_1/W_1/O_2/W_2$ multiple emulsion solvent evaporation method (Scheme 1). Magnetite nanoparticles (Fe_3O_4) were synthesized by co-precipitation method according to Mahdavian et al. [39] report. Glycerine was used as a surfactant to stabilize the dispersed phase. First, to prepare a primary organic phase, 20 mg of magnetic nanoparticles was dispersed in 0.5 ml of dichloromethane (DCM) using a probe ultrasonic (O_1). Next, 5 mg of GO was dispersed in 1.5 ml of deionized water and then 10 mg of 5-Fu, as a hydrophilic drug and 15 mg Tween60, as a surfactant, were added to inner aqueous solution (W_1). Organic solution of the polymer was prepared by dissolving 50 mg PLGA and 250 mg Span60 in 6 ml DCM (O_2). Finally, a W2 aqueous solution was prepared of 150 mg Tween 60 dissolved in 7.5 ml of deionized water (DW) and 7.5 ml of glycerine. The magnetic dispersion was emulsified in the inner aqueous solution by ultrasonication using the sonicator at an output of 50 W for 30 s in an ice-bath, to obtain an O_1/W_1 emulsion. This primary emulsion

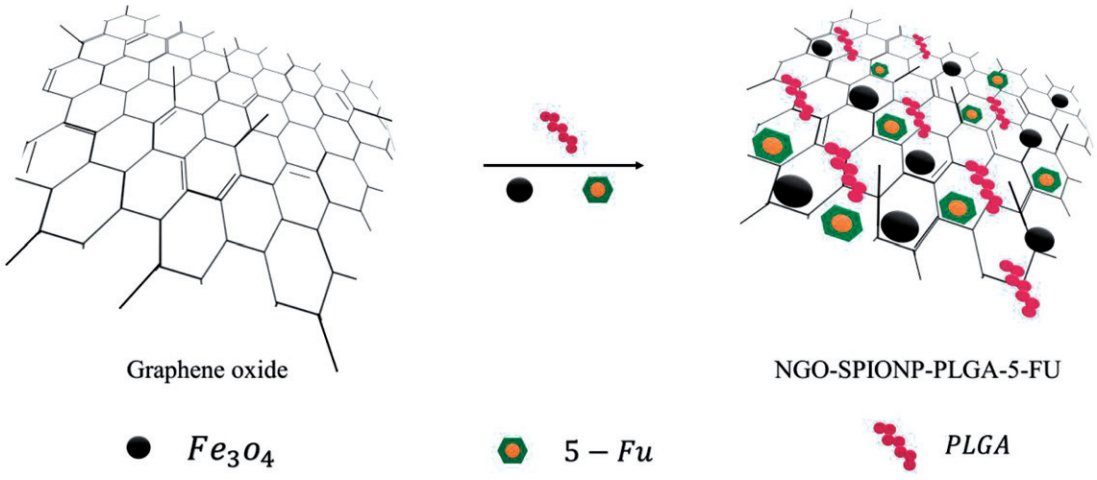

Scheme 1. Schematic representation for the synthesis of NGO-SPION-PLGA-5-Fu.

was emulsified in an organic solution (O_2) of the polymer by ultrasonication for 30 s (50 W) in an ice-bath, to obtain an $O_1/W_1/O_2$ double emulsion. This double emulsion was immediately poured into W_2 aqueous solution and the mixture was ultrasonicated again for 30 s. Consequently, the multiple emulsion ($O_1/W_1/O_2/W_2$) was diluted in 24 ml of aqueous solution containing 12 ml DW and 12 ml glycerine under mechanical stirring for 3 h, and the DCM was removed by solvent evaporation. Finally, the resulting nanoparticles were washed by centrifugation and re-suspension in DW three times and freeze-dried using Tajhizat Sazan Pishtaz Co, automatic freeze-dryer (Iran). In addition, magnetic NGO–PLGA nanoparticles were prepared using a similar technique, while the inner aqueous solution (W_1) was made in the same way, but without 5-Fu.

Characterization of nanoparticles

Dynamic light scattering analysis was used to characterize the hydrodynamic size and effective diameter of nanoparticles. Also, the surface charge of the nanoparticles was investigated by zeta potential measurement. The morphological investigation of nanoparticles was obtained using transmission electron microscope (TEM).

Drug content and encapsulation efficiency

To estimate the drug concentration in nanoparticles, a UV absorption measurement was performed. First, a known quantity of the nanocapsules was weighed and re-dissolved in acetone. Next, the insoluble magnetite particles were removed from the solution by magnetic separation. Finally, the 5-Fu concentration in the acetone solution was determined by UV absorption at a wavelength of 265 nm (the characteristic absorption band of 5-Fu), and the amount of loading and encapsulated drug in the nanocapsules were calculated using Equations (1) and (2).

$$\text{Encapsulation efficiency} = \frac{\text{Amount of } 5-\text{Fu in the nanoparticles}}{\text{Total amount of } 5-\text{fu in dispersion}} \times 100 \quad (1)$$

$$\text{Drug loading efficiency} = \frac{\text{Amount of } 5-\text{Fu in the nanoparticles}}{\text{nanoparticles weight}} \times 100 \quad (2)$$

Also, survival was monitored daily and analysed using Kaplan–Meier survival curves.

In vitro *release study*

The 5-Fu-loaded NGO-SPION-PLGA nanoparticles were transferred to phosphate buffered saline solutions (pH 7.4) (7 mg/mL) in a dialysis bag to evaluate the *in vitro* 5-Fu release from NPs. The dialysis bag was placed fully into the release medium (PBS) and incubated at 37 °C at the shaking speed of 100 rpm. At appropriate time intervals (0, 1, 2, 3, 4, 6, 8, 12, 24, 48, 72, 96, 120–432 h) 2 ml aliquots were withdrawn and replaced with an equal volume of fresh medium. After collecting samples, the concentration of released 5-Fu was analysed using a UV visible spectrophotometer, subjected to signal quantification with the absorption signal at 265 nm. The 5-Fu release kinetics was calculated as a function of time.

In vivo *release study*

A single dose of 5-Fu alone and NGO-SPION-PLGA-5-Fu nanoparticles (5-Fu concentration of 3 mg/kg) was administered intravenously to female rabbits ($n = 6$). Two millilitres of blood samples was collected from rabbit veins at 0.25, 0.5, 1, 2, 4, 8, 24, 96 and 168 h after injection. The samples were extracted from plasma by mixing 250 μL of rabbit plasma with 750 μL of acetonitrile. The mixture was vortexed for 20 s and centrifuged for 10 min at 4000 rpm; 500 μL of supernatant were dried under the steam of N_2 at 87 °C, and the residue was dissolved in 150 μL of DW. Seventy microlitre of the obtained solution was injected into the high-performance liquid chromatography (HPLC). A reverse ACE5-C18 (250 × 4.6 mm) column was used with a mobile phase of 0.01 M KH2PO4/DDW and a flow rate of 0.46 ml/min at room temperature. The absorbance at 265 nm was monitored, and *in vivo* release profile was determined accordingly. The linear equation of standard calibration curve of 5-Fu absorbance as a function of 5-Fu concentration was $y = 0.1697x - 4.3$ ($R^2 > 0.998$). The lower limit of detection was 20 ng/mL.

Cell culture experiments

Mouse colon cancer CT26 cells were cultured in RPMI 1640 supplemented with 10% FBS, penicillin (100 units/mL), and streptomycin (100 mg/mL) in 5% CO_2 and 95% air at 37 °C in a humidified incubator. Cells were harvested by trypsinizing cultures with 1 mM EDTA/0.25% trypsin (w/v) in PBS.

Xenograft tumour mouse model

Male BALB/c mice (6–8 weeks old, 20–30 g) were housed under controlled light, temperature and humidity conditions for one week before use. All animal procedures were carried out in accordance with the institutional Animal Care Committee guidelines (approved by the Research Council of Iran University of Medical Sciences). CT26 cells (3×10^6) in a 100 μL serum-free RMPI-1640 medium were injected subcutaneously onto the right flank of BALB/c mouse.

In vivo *magnetic drug targeting*

To assess the efficiency of nanocapsule localization in a tumour site during the magnetic drug targeting (MDT) procedure, two tumours were established in a mouse bilaterally (one in the right flank and one in the left flank). The initial coronal and sagittal T2-weighted MR images of the mouse were taken before NPs injection. Then, NGO-SPION-PLGA nanoparticles were injected i.v. into the tail vein of the mouse with concentration of 1.2 mg in 100 μL (0.28 mg Fe_3O_4 in 100 μL). For targeting the NPs, the left tumour of the mouse was exposed to an external magnetic field of 0.18 T for 2 h (without applying to another tumour). Next, the same images

were scanned again for both tumours. MR images were obtained with a 3 Tesla MRI scanner and the following parameters were used: TR: 6000 ms, TE: 85 ms, FA: 150°.

Laser irradiation and temperature measurement study

NGO-SPION-PLGA suspensions in doubly DW (DDW) (1.2 mg in 100 μL) was injected subcutaneously after 2 h while applying local magnetic field of 0.18 T to the tumour tissue, and irradiated with an 808 nm continuous-wave NIR laser with the power of 0.8 W/cm^2 and a spot size of 6 × 6 mm (exposure time 10 min). The temperature was measured as a function of time with an infra-red (IR) camera as real time.

In vivo *antitumor effect*

The mice were randomly divided into nine groups of five mice, minimizing the differences of weights and tumour sizes in each group. Theses nine groups were: (A) control, (B) magnetic field of 0.18 T, (C) irradiation of 808 nm NIR laser (0.8 W/cm^2, 8 min), (D) magnetic field +5-Fu (3 mg/kg in 100 μL), (E) magnetic field + NGO-SPION-PLGA-5-Fu (1.2 mg in 100 μL containing 3 mg/kg 5-Fu), (F) magnetic field + NGO-SPION-PLGA (1.2 mg in 100 μL), (G) magnetic field + NGO- SPION-PLGA-5-Fu + NIR (0.8 W/cm^2, 3 min), (H) magnetic field + NGO-SPION-PLGA + NIR (0.8 W/cm^2, 3 min), (I) magnetic field +5-Fu + NIR (0.8 W/cm^2, 8 min).

Drug and nanoparticles were injected intravenously into the tail vein of the mice with a 5-Fu concentration of 3 mg/kg. After injection, in magnetic field group, a magnetic field of 0.18 T was applied to the tumour for 2 h, and finally in groups with NIR, the tumours were irradiated with an 808 nm continuous-wave NIR laser with the power of 0.8 W/cm^2 to obtain 43 °C (3-min and 8-min exposure for with and without NPs injection, respectively). After treatment, tumour size was measured in two dimensions by a caliper every 3 days, and tumour volume (V) was calculated using Equation (3).

$$V = \frac{\text{tumor width}^2}{2} \times \text{tumor length} \quad (3)$$

Statistical analysis

All experiments were performed in triplicate and data are presented as mean ± SD. The tumour growth suppression effect of the various treatment was analysed using one-way analysis of variance. $p < .05$ was considered as statistically significant.

Results

Nanoparticles characterization

The morphology of synthesized NGO-SPION-PLGA and NGO-SPION-PLGA-5-Fu was observed using TEM images (Figure 1), which showed the intact structures of GO sheets. Table 1 shows the size distribution and zeta potential values of nanoparticles of NGO-SPION-PLGA and NGO-SPION-PLGA-5-Fu. The drug loading content and encapsulation efficiency of NGO-SPION-PLGA-5-Fu was 5% and 50%, respectively.

In vitro *release study*

In vitro release of 5-Fu from NGO-SPION-PLGA-5-Fu was carried out in a buffer solution (Figure 2). The results showed the notable prolongation release of 5-Fu. At 37 °C, the initial release within the first 24 h was comparatively quick and

Table 1. Size and surface charge of nanoparticles.

Nanoparticle	Size (nm)	Zeta potential (mV)
NGO-SPION-PLGA	19.2	−32.92 ± 1.04
NGO-SPION-PLGA-5-Fu	72.9	−30.82 ± 0.57

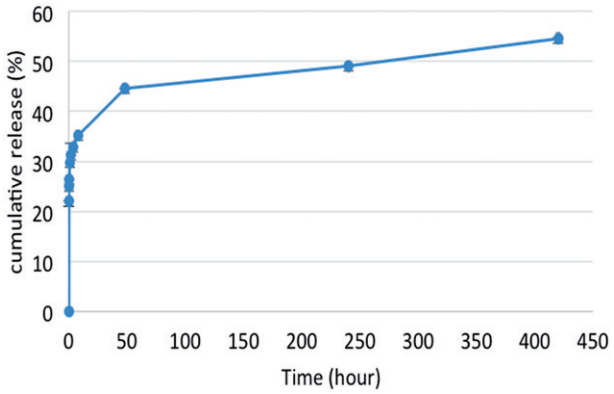

Figure 2. The *in vitro* release profile of 5-Fu from NGO-SPION-PLGA-5-Fu. The plot represents the mean ± standard deviation of the results.

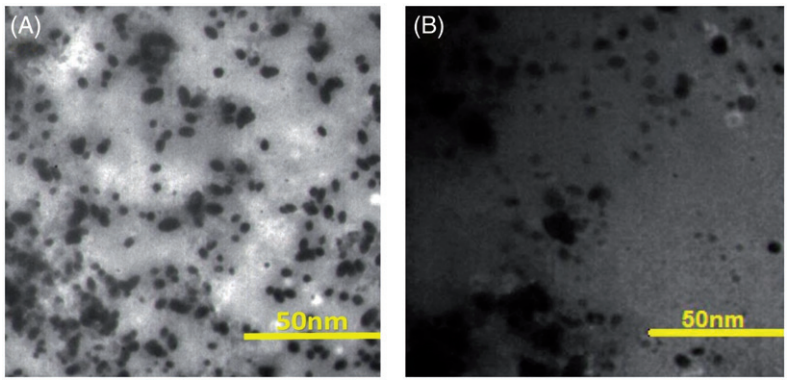

Figure 1. TEM images of the nanoparticles: (A) NGO-SPION-PLGA and (B) NGO-SPION-PLGA-5-Fu.

41.36% of loaded 5-Fu was released in 24 h. Then, continuous and sustained release was observed over 16 days (54.6% total release).

In vivo *release study*

The half-life of 5-Fu in plasma circulation is very short, approximately 8–20 min, therefore many reports have developed 5-Fu preparations with a prolonged lifetime. To study the *in vivo* characteristics of the NGO-SPION-PLGA-5-Fu nanoparticles, we administered 5-Fu alone and NGO-SPION-PLGA-5-Fu nanoparticles to rabbits at a single 5-Fu dose of 3 mg/kg. Figure 3, illustrating 5-Fu alone followed a one-compartment model. Nevertheless, the nanoparticles followed a multi-compartment model, including burst release and sustained release. The nanoparticles showed lower peak concentration of 5-Fu as compared with free 5-Fu solution, and high drug level was detected up to 4 h because of sustained release of 5-Fu from the nanoparticles. Consequently, our complex has a higher removal half-life.

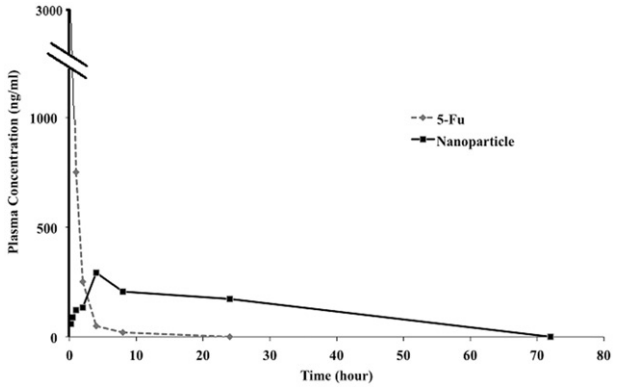

Figure 3. The mean plasma concentrations of 5-Fu following i.v. administration of 5-Fu and NGO-SPION-PLGA-5-Fu nanoparticles at a 5-Fu dose of 3 mg/kg.

In vivo *magnetic drug targeting*

Figure 4 shows T2-weighted MR images of CT-26 tumours implanted in mice before and 2 h after nanoparticles injection with concentration of 1.2 mg in 100 μL. After i.v. injection of magnetic nanoparticles, a permanent magnetic field of 0.18 T was placed above the left tumour for 120 min. In T2-weighted fast spin echo images, accumulation of magnetic nanoparticles in the tumour was seen as dark regions, showing that NGO-SPION-PLGA nanoparticles were accurately targeted to the desired location under the aid of an external magnetic field and not systemically distributed.

Laser irradiation and temperature measurement study

In this study, the main objective of increasing temperature is reaching 43 °C. Before irradiation, the average of initial temperature inside the tumours was 34.2 ± 1.2 °C and interstitial temperature was increased in time-dependent methods. Figure 5(A) shows the effect of photothermal treatment using an 808 nm laser by an IR thermal imaging system. Figure 5(B) shows the increasing temperature profiles of the tumours during the exposure time. The *in vivo* experiments demonstrated that the presence of nanoparticles significantly enhances NIR-induced heat generation. The mean temperature of tumours exposed to NIR alone was increased up to 43.5 ± 0.65 °C at 8 min. It was confirmed that administration of NGO-SPION-PLGA and subsequent NIR irradiation heated the CT26 tumours up to 43.3 ± 0.52 °C at 3 min.

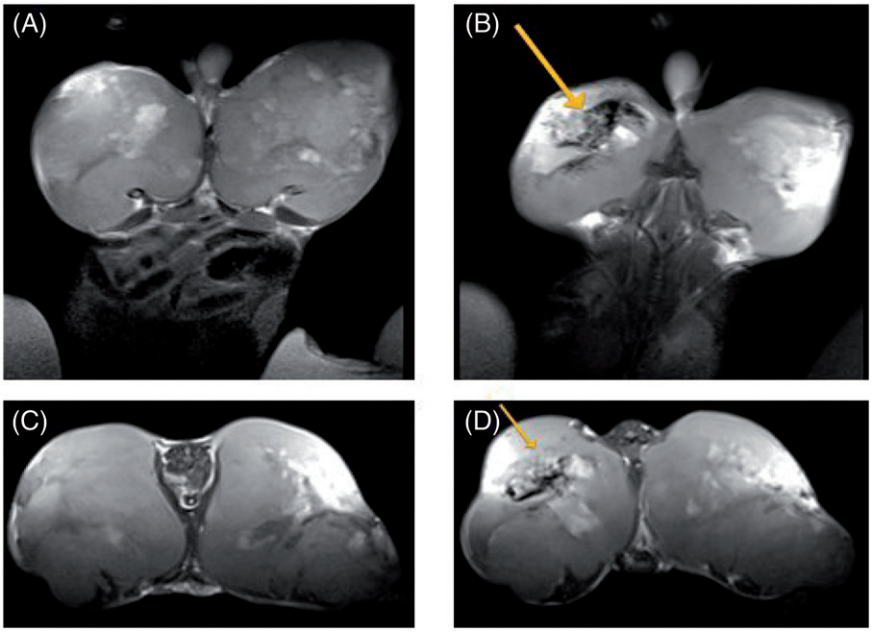

Figure 4. MRI scans of the mouse implanted with colon cancer (CT26 cell line): (A and C) coronal and sagittal scans before the injection of NPs and (B and D) coronal and sagittal scans, 120 min after the injection of NGO-SPION-PLGA nanoparticles. The new dark regions in the left tumour (indicated with an arrow) show the accumulation of magnetic-NGO after the application of a magnetic field.

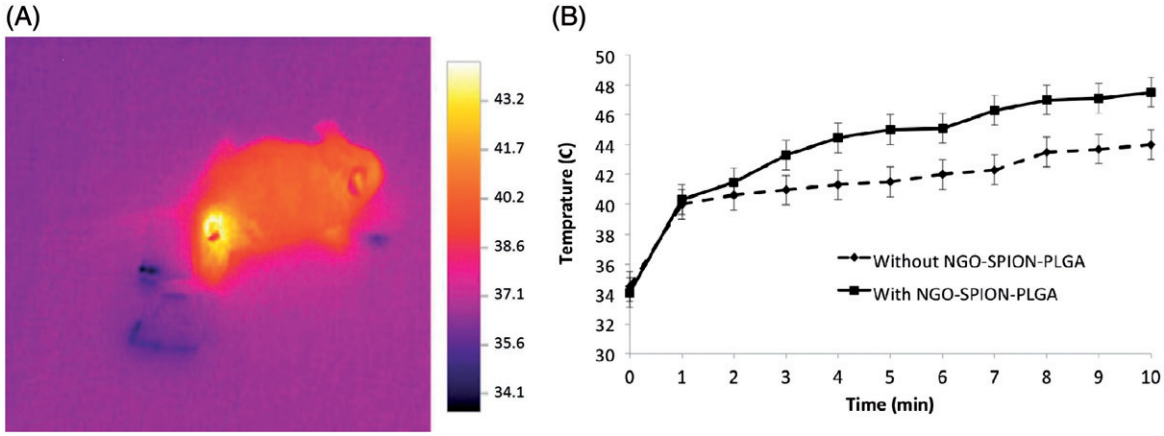

Figure 5. Laser irradiation and temperature measurement. (A) Effect of photothermal treatment using an 808 nm laser by an IR thermal imaging system. (B) Temperature changes by NIR (808 nm, 0.8 w/cm^2) with and without NGO-SPION-PLGA as a function of time in mice implanted with colon cancer.

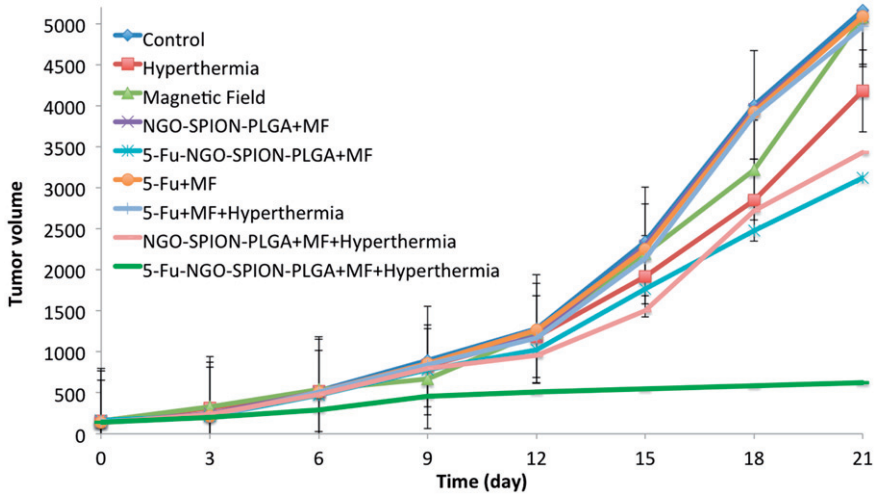

Figure 6. Tumour growth suppression effects of various treatment protocols against CT26 tumour. The data represent the means ± SD, $n = 3$.

In vivo *antitumor effect*

The efficacy of our nanocarriers in colon-bearing mice was investigated in terms of tumour volume (mm3). Mice were treated as mentioned in the "Materials and methods" section to assess the therapeutic effects of NPs containing 5-Fu *in vivo*. Figure 6 shows the effect of various treatment protocols on CT26 tumour growth in Balb/c. There were no significant differences between groups A (control), B (magnet), C (NIR), D (NGO-SPION-PLGA + magnet), E (5-Fu + magnet + NIR), and F (5-Fu + magnet) 21 days after start of treatments ($p > .05$). However, there were significant differences ($p < .01$) between group A (control), G (NGO-SPION-PLGA-5-Fu + magnet), H (NGO-SPION-PLGA-5-Fu + magnet + NIR), and I (NGO-SPION-PLGA + magnet + NIR). Our results showed that the average tumour volume after treatment in group H was smaller compared with the other treatment groups. In addition, the rank of median survival time was NGO-SPION-PLGA-5-Fu + magnet (36 day)> NGO-SPION-PLGA + magnet + NIR (30 day)> magnet+ 5-Fu + NIR (29 day)> Magnet+ 5-Fu (28 day) > NGO-SPION-PLGA + magnet (26 day)> NIR (25 day) > Magnet (24 day)> Control (23 day) at 40 days follow up. By the log-rank test, the median survival time NGO-SPION-PLGA-5-Fu + magnet + NIR was significantly prolonged compared to the rest ($p < .05$) (Figure 7(A)). Figure 7(B) shows the images of tumours on mice after various treatments. The tumour was suppressed with 5-Fu-NGO-SPION-PLGA treatment in combined with laser irradiation.

Discussion

In the present study, NGO-SPION-PLGA nanoparticles have been expended for the delivery of hydrophilic drug. Nano-GO was negatively charged because of the presence of a large number of –COOH groups [11]. Table 1 shows the characteristics of NGO-SPION-PLGA and NGO-SPION-PLGA-5-Fu nanoparticles.

Clinically, 5-Fu can be administered by continuous infusion, which mostly prevents DNA synthesis, or by bolus injection, which mostly prevents RNA synthesis [40]. Because 5-Fu is quickly metabolized in the body, a continuous high dose is required to sustain a therapeutic serum level. Our results indicated that when 5-Fu is loaded into nanoparticles, the 5-Fu has a prolonged half-life and sustained-release. The *in vitro* release was slow and only 54.6% of loaded 5-Fu was released within 16 days (Figure 2), which is almost similar to other studies [41,42]. It is worth noting that the pharmacokinetic

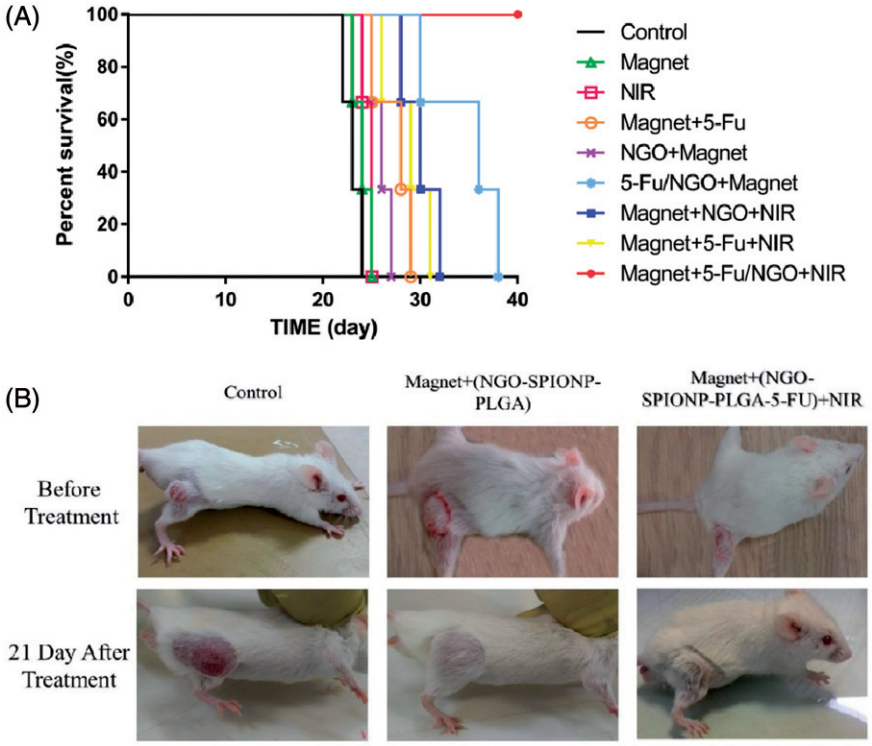

Figure 7. Effect of various treatments on survival of mice. (A) Kaplan–Meier survival curves of control and treated mice. (B) Representative photographs of tumours on mice after various treatments.

characteristics of our 5-Fu-loaded NGO-SPION-PLGA nanoparticles are approximately similar to the 5-Fu-loaded magnetic PLGA nanoparticles of Shakeri-Zadeh et al. [43]. Based on Figure 3, it is seen that when 5-Fu alone is administrated, the plasma concentration of 5-Fu is rapidly decreased within 4 h, whereas 5-Fu concentration in rabbit plasma increases and then starts decreasing within 24 h in NGO-SPION-PLGA-5-Fu administration. Hence, our *in vivo* studies indicate that when 5-Fu is loaded into NGO-SPION-PLGA nanoparticles, the 5-Fu has a sustained release. It is remarkable that the pharmacokinetic characteristics of our 5-Fu-loaded NGO-SPION-PLGA nanoparticles are similar to the 5-Fu-loaded 5-Fu/PEG-PBLG nanoparticles of Li et al. [44].

In the case of photothermal treatment using an 808-nm laser, we measured the real-time temperature changes of the tumour tissue by an IR thermal imaging system (Figure 5(A)). The NGO-SPION-PLGA nanoparticles may be effective thermal generators, which could absorb NIR by the NGO and SPION (Fe_3O_4) ingredients; these results are confirmed by studies [45–47]. As a comparison, our colleagues reached temperature increasing by PTT treatment using a dose of 80 μg/mL of nanographene oxide and 2 min of laser exposure with the power of 2 W/cm^2 *in vitro*.

Absorbed NIR promotes molecular alternation, leading to efficient heating of the surrounding environment, which could be employed as thermal ablation agents for thermal destruction of tumours [11]. In mice injected with nanoparticles (after magnetic targeting), the temperature of the tumour started to increase as soon as laser irradiation began and the temperature reached to 43 °C after 3 min of laser exposure (Figure 5(B)). Whereas mice (without nanoparticles injection) were treated with the same laser, temperature increasing to 43 °C was observed in 8 min. It demonstrated the excessive cumulating of NGO-SPION-PLGA inside the tumour tissue and its capability to induce hyperthermia by converting NIR light energy to heat *in vivo*. After the laser treatments, mice were observed for 21 days; during this period no mice died. This suggests that the i.v. injection of nanoparticles was not significantly toxic to the mice. The size of tumour was significantly suppressed in mice treated with NGO-SPION-PLGA-5-Fu + magnetic field + NIR. One obvious observation was that there were black round indications on the mice skins, a direct evidence of the tumour necrosis, and this is due to origination of the extreme local heating from NGO-SPION-PLGA by NIR laser irradiation (Figure 7). Quantitative measurements showed that tumour volume increased rapidly in the control groups, from about 140 mm3 to approximately 5000 mm^3. Strikingly, combined treatment of the NGO-SPION-PLGA and NIR irradiation suppressed the tumour within 21 days. The results suggested that the NGO-SPION-PLGA-5-Fu nanoparticle was an effective agent for *in vivo* PTT of cancer. Preceding reports have confirmed that complete tumour ablation could be reached by PTT treatment using NGO; the results were achieved using a high dose of NGO and longer exposure to laser. As a comparison, Zhang et al. reached a thorough tumour ablation by PTT treatment using a dose of 10 mg/kg of nanographene oxide and 5 min of laser exposure [2]. In contrast, the present study reduced the dose of nanoparticles to 3 mg/kg and the laser irradiation was performed for 3 min.

In addition, owing to the presence of iron oxide, our nanoparticles appeared in MRI images as dark regions that verify the theranostic effect. Meanwhile, early reports have proven this result [48,49]. The results demonstrate that combining

two therapeutic approaches into one system allowed us to reduce the dose of nanoparticle as well as 5-Fu significantly, but still achieved a highly efficient therapeutic performance. Thus, we predict that NGO-SPION-PLGA mediated delivery of 5-Fu and combined phototherapy is a promising approach for efficient tumour suppression.

Conclusions

In this study, we prepared 5-Fu-loaded NGO-SPION-PLGA nanoparticles, which exhibited favourable pharmacokinetic characteristics, including sustained drug release and prolonged drug half-life. *In vivo*, NGO-SPION-PLGA-5-Fu nanoparticles had good anti-tumour activity against colon cancer xenografts. Taken together, our results indicate that a NGO nanoparticle delivery system for 5-Fu may be able to effectively reduce contrary side effects of 5-Fu therapy and develop the therapeutic index of 5-Fu. Consequently, in the *in vivo* studies, NGO-SPION-PLGA-5-Fu showed excellent PTT efficacy, magnetic targeting property, and MRI ability, indicating that there is a great potential of NGO-SPION-PLGA-5-Fu for cancer theranostic applications.

Disclosure statement

The authors report no conflicts of interest. The authors alone are responsible for the content and writing of the paper.

Funding

This research was supported by grant No. [27448] from the School of Medicine, Iran University of Medical Sciences (IUMS).

References

[1] Tsung-Ju L, Chih-Chia H, Pin-Wei R, et al. In vivo anti-cancer efficacy of magnetite nanocrystal-based system using locoregional hyperthermia combined with 5-fluorouracil chemotherapy. Biomaterials. 2013;34:7873–7883.
[2] Wen Z, Zhouyi G, Deqiu H, et al. Synergistic effect of chemo-photothermal therapy using PEGylated graphene oxide. Biomaterials. 2011;32:8555–8561.
[3] Poliraju K, Raviraj V, Chi-Shiun C, et al. Nano-graphene oxide-mediated In vivo fluorescence imaging and bimodal photodynamic and photothermal destruction of tumors. Biomaterials. 2016;95:1–10.
[4] Phillips D. Light relief: photochemistry and medicine. Photochem Photobiol Sci. 2010;9:1589–1596.
[5] Huiyul P, Jaemoon Y, Jaemin L, et al. Multifunctional nanoparticles for combined doxorubicin and photothermal treatments. ACS Nano. 2009;3:2919–2926.
[6] Hildebrandt B. The cellular and molecular basis of hyperthermia. Crit Rev Oncol/Hematol. 2002;43:33–56.
[7] Ho Sang J, Won Ho K, Dong Kyung S, et al. Nanographene oxide–hyaluronic acid conjugate for photothermal ablation therapy of skin cancer. ACS Nano. 2014;8:260–268.
[8] Shenglin L, Zhangyou Y, Xu T, et al. Multifunctional photosensitizer grafted on polyethylene glycol and polyethylenimine dual-functionalized nanographene oxide for cancer-targeted near-infrared imaging and synergistic phototherapy. ACS Appl Mater Interfaces. 2016;8:17176–17186.
[9] Kai Y, Jianmei W, Shuai Z, et al. The influence of surface chemistry and size of nanoscale graphene oxide on photothermal therapy of cancer using ultra-low laser power. Biomaterials. 2012;33:2206–2214.
[10] Kai Y, Shuai Z, Guoxin Z, et al. Graphene in mice: ultrahigh in vivo tumor uptake and efficient photothermal therapy. Nano Lett. 2010;10:3318–3323.
[11] Abhishek S, Won Il C, Jong Hyun L, et al. Graphene oxide mediated delivery of methylene blue for combined photodynamic and photothermal therapy. Biomaterials. 2013;34:6239–6248.
[12] Liangzhu F, Xianzhu Y, Xiaoze S, et al. Polyethylene glycol and polyethylenimine dual-functionalized nano-graphene oxide for photothermally enhanced gene delivery. Small. 2013;9:1989–1997.
[13] Bo T, Chao W, Shuai Z, et al. Photothermally enhanced photodynamic therapy delivered by nano-graphene oxide. ACS Nano. 2011;5:7000–7009.
[14] Kai Y, Liangzhu F, Xiaoze S, et al. Nano-graphene in biomedicine: theranostic applications. Chem Soc Rev. 2013;42:530–547.
[15] Huang P, Xu C, Lin J, et al. Folic acid-conjugated graphene oxide loaded with photosensitizers for targeting photodynamic therapy. Theranostics. 2011;1:240.
[16] Xiaoying Y, Xiaoyan Z, Zunfeng L, et al. High-efficiency loading and controlled release of doxorubicin hydrochloride on graphene oxide. J Phys Chem C. 2008;112:17554–17558.
[17] Zoran M, Ljubica MH, Biljana MT, et al. In vitro comparison of the photothermal anticancer activity of graphene nanoparticles and carbon nanotubes. Biomaterials. 2011;32:1121–1129.
[18] Hung-Wei Y, Yu-Jen L, Kun-Ju L, et al. EGRF conjugated PEGylated nanographene oxide for targeted chemotherapy and photothermal therapy. Biomaterials. 2013;34:7204–7214.
[19] Haiqing D, Chunyan D, Tianbin R, et al. Surface-engineered graphene-based nanomaterials for drug delivery. J Biomed Nanotechnol. 2014;10:2086–2106.
[20] Nenad I, Victoria W, Zorica A, et al. Chitosan-PLGA polymer blends as coatings for hydroxyapatite nanoparticles and their effect on antimicrobial properties, osteoconductivity and regeneration of osseous tissues. Mater Sci Eng C Mater Biol Appl. 2016;60:357–364.
[21] Kim DH, Martin DC. Sustained release of dexamethasone from hydrophilic matrices using PLGA nanoparticles for neural drug delivery. Biomaterials. 2006;27:3031–3037.
[22] Zhang L, Zhang L. Lipid–polymer hybrid nanoparticles: synthesis, characterization and applications. Nano Life. 2010;01:163–173.
[23] Acharya S, Sahoo SK. PLGA nanoparticles containing various anticancer agents and tumour delivery by EPR effect. Adv Drug Deliv Rev. 2011;63:170–183.
[24] Azeem A, Bin Y, Alison SB, et al. Convection-enhanced delivery of carboplatin PLGA nanoparticles for the treatment of glioblastoma. PLoS One. 2015;10:e0132266.
[25] Anitha MT, Anita IK, Jennifer IH, et al. Development of a liposomal nanoparticle formulation of 5-fluorouracil for parenteral administration: formulation design, pharmacokinetics and efficacy. J Control Release. 2011;150:212–219.
[26] Zinutti C. In-vivo evaluation of sustained release microspheres of 5-FU in rabbits. Int J Pharma. 1998;166:231–234.
[27] Ashish G, Vaibhav P, Rajeev S, et al. Heparin-appended polycaprolactone core/corona nanoparticles for site specific delivery of 5-fluorouracil. Artif Cells, Nanomed Biotechnol. 2017;45:1146–1155.
[28] Taegyu K, Fangyuan L, Seungmin B, et al. Surface design of magnetic nanoparticles for stimuli-responsive cancer imaging and therapy. Biomaterials. 2017;136:98–114.
[29] Brigger I, Dubernet C, Couvreur P. Nanoparticles in cancer therapy and diagnosis. Adv Drug Deliv Rev. 2002;54:631–651.
[30] Ziyong C, Yunlu D, Xiaojiao K, et al. Gelatin-encapsulated iron oxide nanoparticles for platinum (IV) prodrug delivery, enzyme-stimulated release and MRI. Biomaterials. 2014;35:6359–6368.
[31] Zhongling W, Ruirui Q, Na T, et al. Active targeting theranostic iron oxide nanoparticles for MRI and magnetic resonance-guided focused ultrasound ablation of lung cancer. Biomaterials. 2017;127:25–35.
[32] Oghabian MA., Jeddi-Tehrani M, Zolfaghari A, et al. Detectability of Her2 positive tumors using monoclonal antibody conjugated

iron oxide nanoparticles in MRI. J Nanosci Nanotechnol. 2011;11:5340–5344.
[33] Xiujuan F, Guozheng J, Wei Z, et al. Magnetic Fe 3 O 4–graphene composites as targeted drug nanocarriers for pH-activated release. Nanoscale. 2013;5:1143–1152.
[34] Costas GH, Michael JB, Srinivasan B, et al. Metallic iron nanoparticles for MRI contrast enhancement and local hyperthermia. Small. 2008;4:1925–1929.
[35] Ilaria M, Francesca A, Stefania B, et al. Synthesis of lipophilic core–Shell Fe3O4@ SiO2@ Au nanoparticles and polymeric entrapment into nanomicelles: a novel nanosystem for in vivo active targeting and magnetic resonance–photoacoustic dual imaging. Bioconjugate Chem. 2017;28:1382–1390.
[36] Kai Y, Lilei H, Xingxing M, et al. Multimodal imaging guided photothermal therapy using functionalized graphene nanosheets anchored with magnetic nanoparticles. Adv Mater. 2012;24:1867–1872.
[37] Jin-Sil C, Young-Wook J, Soo-In Y, et al. Biocompatible heterostructured nanoparticles for multimodal biological detection. J Am Chem Soc. 2006;128:15982–15983.
[38] Minhong J, Seongtae B, Asahi T, et al. Effects of particle dipole interaction on the ac magnetically induced heating characteristics of ferrite nanoparticles for hyperthermia. Appl Phys Lett. 2009;95:082501.
[39] Mahdavian AR, Mirrahimi MA-S. Efficient separation of heavy metal cations by anchoring polyacrylic acid on superparamagnetic magnetite nanoparticles through surface modification. Chem Eng J. 2010;159:264–271.
[40] Samira E, Samideh K, Sepideh K, et al. Evaluation of the cytotoxic effects of hyperthermia and 5-fluorouracil-loaded magnetic nanoparticles on human colon cancer cell line HT-29. Int J Hyperthermia. 2017;33:327–335.
[41] Ashjari M, Khoee S, Mahdavian AR. A multiple emulsion method for loading 5-fluorouracil into a magnetite-loaded nanocapsule: a physicochemical investigation. Polym Int. 2012;61:850–859.
[42] Wang G, Chen G, Wei Z, et al. *Multifunctional Fe 3 O 4/graphene oxide nanocomposites for magnetic resonance imaging and drug delivery*. Materials Chemistry and Physics. 2013;141:997–1004.
[43] Ali S, Mohammad-Bagher S, Sepideh K, et al. A new magnetic nanocapsule containing 5-fluorouracil: in vivo drug release, antitumor, and pro-apoptotic effects on CT26 cells allograft model. J Biomater Appl. 2014;29:548–556.
[44] Su L, Anxun W, Wenqi J, et al. Pharmacokinetic characteristics and anticancer effects of 5-fluorouracil loaded nanoparticles. BMC Cancer. 2008;8:103.
[45] Kargar S, Khoei S, Khoee S, et al. Evaluation of the combined effect of NIR laser and ionizing radiation on cellular damages induced by IUdR-loaded PLGA-coated nano-graphene oxide. Photodiagn Photodynamic Ther. 2018;21:91–97.
[46] Mirrahimi M, et al. Selective heat generation in cancer cells using a combination of 808 nm laser irradiation and the folate-conjugated Fe2O3@ Au nanocomplex. Artif Cells Nanomed, Biotechnol. 2018. [Epub ahead of print]. doi: 10.1080/21691401.2017.142007
[47] Hung-Wei Y, Mu-Yi H, Tsong-Long H, et al. Non-invasive synergistic treatment of brain tumors by targeted chemotherapeutic delivery and amplified focused ultrasound-hyperthermia using magnetic nanographene oxide. Adv Mater. 2013;25:3605–3611.
[48] Mulan L, Hoe Suk K, Lianji T, et al. Comparison of two ultrasmall superparamagnetic iron oxides on cytotoxicity and MR imaging of tumors. Theranostics. 2012;2:76.
[49] Ming W, Qingtang W, Da Z, et al. Magnetite nanocluster@ poly (dopamine)-PEG@ indocyanine green nanobead with magnetic field-targeting enhanced MR imaging and photothermal therapy in vivo. Colloids Surf B Biointerfaces. 2016;141:467–475.